Supplementary Information

Structural Disorder and Coherence across the Phase Transitions of Lead-Free Piezoelectric $Bi_{0.5}K_{0.5}TiO_3$

Bo Jiang[1], Trygve M. Raeder[1], De-Ye Lin[2], Tor Grande[1] and Sverre M. Selbach[1*]

[1]Department of Materials Science and Engineering,

NTNU – Norwegian University of Science and Technology, 7491 Trondheim, Norway.

[2]CAEP software Center for High Performance Numerical Simulation, Institute of Applied Physics and Computational Mathematics, Huayuan road 6, Beijing 100088, P.R. China

*Correspondence should be addressed to selbach@ntnu.no

Additional Experimental and Computational Details

Rietveld refinement of reciprocal space diffraction patterns was done with the General Structure Analysis System (GSAS) [1] program. The scale factor, zero shift, background, unit cell parameters, peak profile parameters and isotropic temperature factors were refined.

The PDF G(r) gives the probability of finding an atom at a distance of *r* (radial distance) from a given atom [2, 3], $G(r)=4\pi[\rho(r)-\rho_0]$, where ρ(r) and ρ_0 correspond to the local and average atomic number density, respectively, and the intensity of G(*r*) is determined by the number of pairs of atoms. The G(r) is obtained by Fourier transform of the normalized total structure function S(Q), $G(r) = \frac{2}{\pi}\int_0^\infty Q[S(Q)-1]\sin(Qr)dQ$, where Q is the magnitude of the scattering vector ($Q=4\pi\sin\theta/\lambda$). The total scattering from both Bragg scattering and diffuse scattering are obtained simultaneously and included in S(Q). PDF G(r) were obtained with the PDFgetX3 software [4] using a Q_{max} of 22.8 $Å^{-1}$. PDF patterns were analyzed both by small-box modeling using PDFgui [5], and by large-box Reverse Monte Carlo (RMC) modeling using RMCprofile [6], where the total structure function S(Q), G(r) and Bragg peaks were fitted simultaneously. The Rietveld refined structure was used as starting parameters in PDFgui modeling, and the scale factor, lattice constants, atomic positions and atomic displacement parameters (ADP) were refined. Each RMC simulation ran for 24 hours on one 3.1GHz CPU core, generating about 2.0×10^6 moves in a 12×12×12 supercell containing 8640 atoms. Bond valence sum (BVS) restrictions were applied to avoid unphysical bond lengths, and Bi^{3+} and K^+ were allowed to swap places on the A-site sublattice.

Additional results from Rietveld and PDFgui refinements

Table S1. Results of the Rietveld refinements with space group *P*4*mm* and a mixed A-site model of BKT from room temperature to 773K.

	300K	323K	373K	423K	473K	523K
a(Å)	3.9206(4)	3.9216(3)	3.9239(3)	3.9265(3)	3.9297(3)	3.9332(3)
c(Å)	3.9723(5)	3.9725(5)	3.9715(4)	3.9697(4)	3.9665(4)	3.9623(4)
c/a	1.0132	1.0130	1.0121	1.0110	1.0094	1.0074
vol(Å^3)	61.05	61.09	61.14	61.20	61.25	61.29
z(Ti)	0.558(1)	0.556(1)	0.556(1)	0.554(1)	0.552(1)	0.550(1)
z(O1)	0.134(3)	0.129(4)	0.128(3)	0.124(3)	0.118(3)	0.109(4)
z(O2)	0.600(3)	0.601(3)	0.599(3)	0.598(3)	0.596(3)	0.597(4)
U_{iso}(Bi/K)	0.0482(8)	0.0558(9)	0.0529(8)	0.0565(9)	0.0578(5)	0.0669(9)
U_{iso} (Ti)	0.004(1)	0.008(1)	0.006(1)	0.007(1)	0.006(1)	0.008(1)
U_{iso} (O)	0.006(2)	0.012(3)	0.008(2)	0.009(2)	0.007(3)	0.010(3)
R_{wp}	0.0699	0.0662	0.0658	0.0623	0.0603	0.0551
	573K	623K	673K	723K	773K	
a(Å)	3.9370(2)	3.9411(3)	3.9429(2)	3.9448(3)	3.9465(3)	
c(Å)	3.9575(4)	3.9525(5)	3.9533(4)	3.9540(5)	3.9551(5)	
c/a	1.0052	1.0029	1.0026	1.0023	1.0022	
vol(Å^3)	61.34	61.39	61.45	61.53	61.60	
z(Ti)	0.543(2)	0.538(2)	0.535(2)	0.531(2)	0.527(3)	
z(O1)	0.097(5)	0.086(7)	0.079(8)	0.076(9)	0.07(1)	
z(O2)	0.587(5)	0.592(6)	0.584(7)	0.583(8)	0.582(9)	
U_{iso}(Bi/K)	0.072(1)	0.085(1)	0.086(1)	0.090(1)	0.094(1)	
U_{iso} (Ti)	0.014(1)	0.014(1)	0.015(1)	0.017(1)	0.020(1)	
U_{iso} (O)	0.015(4)	0.013(4)	0.015(4)	0.015(5)	0.016(5)	
R_{wp}	0.0486	0.0488	0.0472	0.0455	0.0443	

Table S2. Results of the real space PDF refinements done in the space group *P*4*mm* of BKT from room temperature to 773 K with fitting range 1.5-80 Å.

	300K	323K	373K	423K	473K	523K
a(Å)	3.9281(4)	3.9293(5)	3.9316(5)	3.9343 (5)	3.9375(5)	3.9411(6)
c(Å)	3.990(1)	3.990 (1)	3.989(1)	3.987(1)	3.984(1)	3.980(1)
c/a	1.016	1.015	1.015	1.013	1.012	1.010
vol(Å^3)	61.57	61.60	61.66	61.71	61.77	61.82
z(Ti)	0.572(2)	0.571(2)	0.570(2)	0.568(2)	0.567(3)	0.565(3)
z(O1)	0.09(1)	0.08(1)	0.08(1)	0.07(1)	0.06(1)	0.05(2)
z(O2)	0.621(7)	0.620(7)	0.618(7)	0.616(8)	0.615(8)	0.612(9)
U_{iso}(Bi/K)	0.053(2)	0.055 (2)	0.058(2)	0.061(2)	0.066(2)	0.071(3)
U_{iso} (Ti)	0.011 (1)	0.012(1)	0.013(1)	0.013(1)	0.014(1)	0.016(1)
U_{iso} (O)	0.046(5)	0.047 (5)	0.048(5)	0.049(5)	0.050(6)	0.051(6)
R_w	0.202	0.196	0.186	0.177	0.170	0.166
	573K	623K	673K	723K	773K	
a(Å)	3.9460(8)	3.950(1)	3.953(1)	3.956 (2)	3.958 (2)	
c(Å)	3.972(1)	3.967(2)	3.965(3)	3.964(4)	3.964(5)	
c/a	1.007	1.004	1.003	1.002	1.002	
vol(Å^3)	61.85	61.90	61.96	62.04	62.12	
z(Ti)	0.562(4)	0.557(4)	0.554(5)	0.552(6)	0.549(6)	
z(O1)	0.03(3)	0.02(3)	0.02(3)	0.02(3)	0.02(4)	
z(O2)	0.60(1)	0.60(1)	0.60(1)	0.60(1)	0.60(1)	
U_{iso}(Bi/K)	0.078(3)	0.083(3)	0.085(4)	0.088(4)	0.089(5)	
U_{iso} (Ti)	0.018(1)	0.021(1)	0.023(2)	0.025(2)	0.026(2)	
U_{iso} (O)	0.050(6)	0.048(7)	0.048(7)	0.048(7)	0.048(8)	
R_w	0.167	0.169	0.168	0.167	0.164	

Thermal evolution of A-site cation ordering

The thermal evolution of local A-site cation ordering can be expressed in terms of the nearest neighbor function n_{ij}(r) [7, 8]. The n_{ij}(r) is defined as the mean number of atoms *i* surrounding a central atom *j*; $n_{ij}(r) = \int_{r2}^{r1} 4\pi r^2 2c_j\rho_0 g_{ij}(r)dr$, where c_j is the proportion of atom j in compound, ρ_0 is the average number density of compounds, and g_{ij} is the partial distribution function for atoms $_i$ and j. The A-site $n_{A\text{-}A}$(r)s derived from the disordered RMC models in Figure 5d in the main text are shown in Figure S1a. For comparison, the A-site $n_{A\text{-}A}$(r) for the mixed A-site random model and ordered models with 001-layered and 111-rock salt configurations of Bi and K on the A-site sublattice are shown in in Figure S1b. For simplicity, no local structural distortions are included in Figure S1b. Each step corresponds to an A-site coordination shell. For a cubic perovskite, there will be 6 neighbors in the first coordination shell and 18 neighbors in the second shell. The degree of cation ordering inferred from the $n_{A\text{-}A}$(r) obtained from RMC simulations shown in Figure S1a indicates that the A-site sublattice with Bi^{3+} and K^+ cations is almost completely disordered at all temperatures considered.

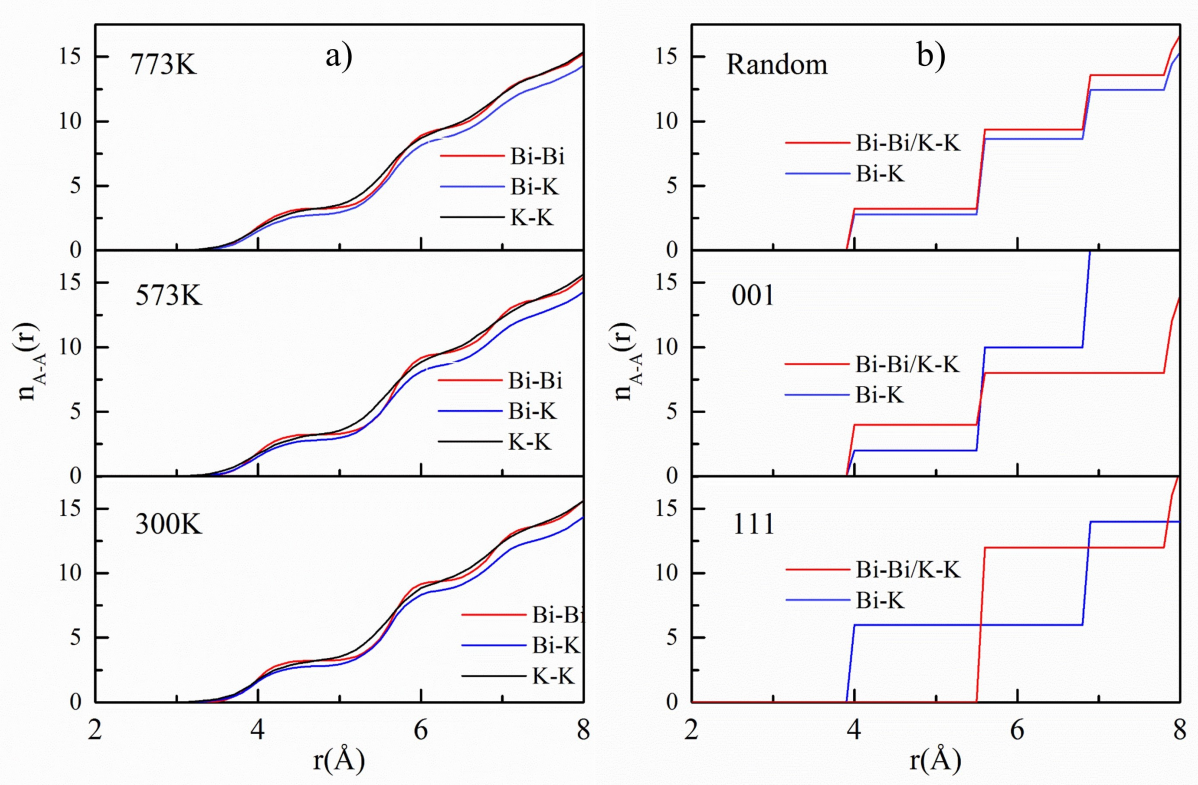

Figure S1. Nearest neighbor functions $n_{A\text{-}A}$(r) show the local short-range order of the A-site cations in BKT at 300K, 573K and 773K for (a) RMC derived disordered model, and from (b) random mixed A-site model and ordered models with 001-layer and 111-rock salt configurations.

Additional results from ab initio molecular dynamics simulations

Snapshots from AIMD simulations for $Bi_{32}K_{32}Ti_{64}O_{192}$ at different temperature are shown in Figure S2. We note that the A-site, B-site and Ti-O octahedra become more distorted with rising temperature, as expected due to increasing thermal vibrations.

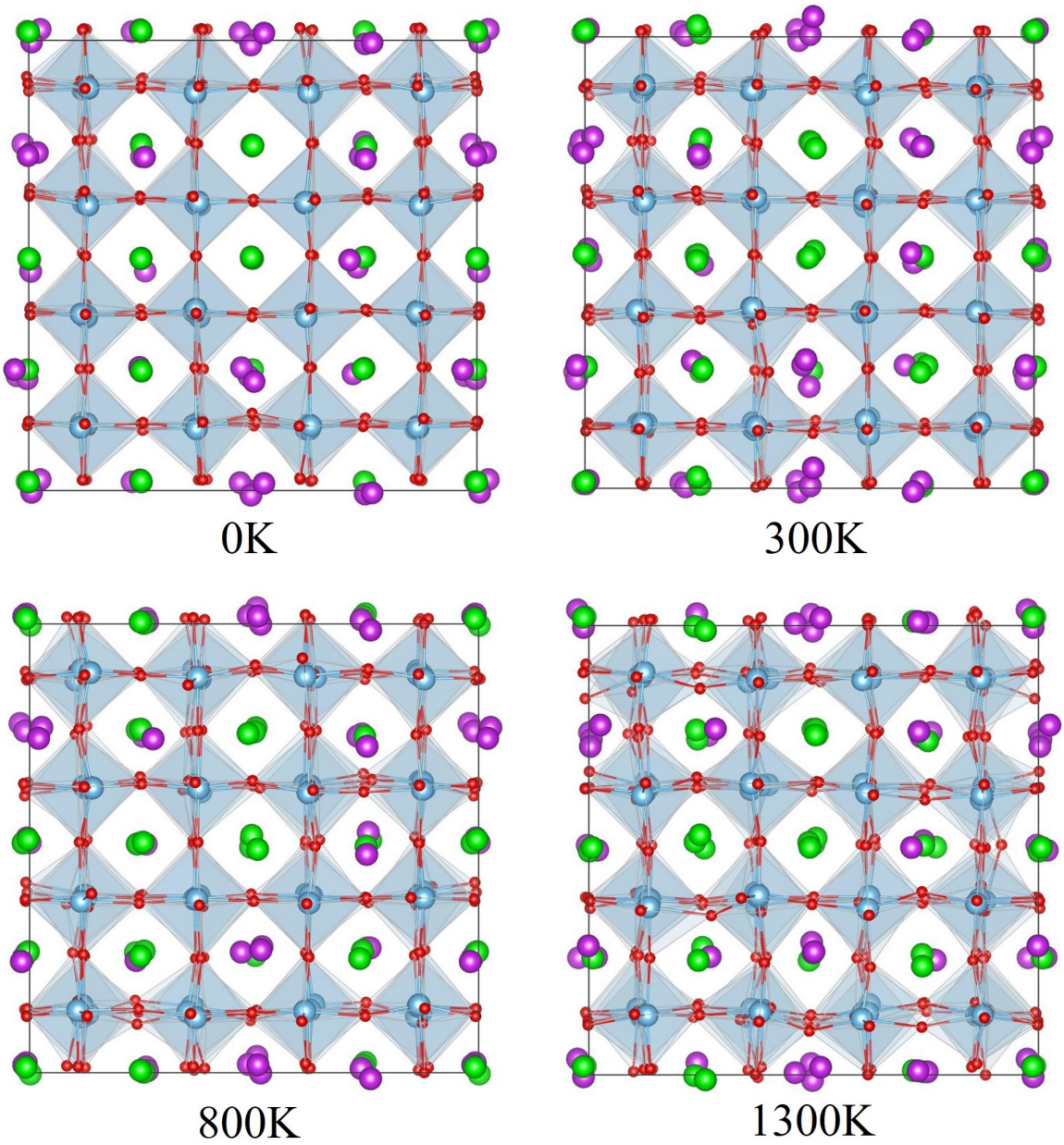

Figure S2. Snapshots from AIMD simulations of the 4×4×4 disordered supercells with 320 atoms at different temperatures after 5000 steps.

References

(1） Larson, A. C.; Dreele, R. B. V., General Structure Analysis System technical manual. *LANSCE, MS–H805 Los Almos National Laboratory LAUR* **2000**, 86-748.
(2） Petkov, V., Nanostructure by high-energy X-ray diffraction. *Mater. Today* **2008,** *11*, 28-38.
(3） Takeshi Egami; Billinge, S., Underneath the Bragg Peaks, Structural Analysis of Complex Materials. *Elsevier: Oxford* **2003,** *7*.
(4） Juhas, P.; Davis, T.; Farrow, C. L.; Billinge, S. J. L., PDFgetX3: a rapid and highly automatable program for processing powder diffraction data into total scattering pair distribution functions. *J. Appl. Crystallogr.* **2013,** *46*, 560-566.
(5） Farrow, C. L.; Juhas, P.; Liu, J. W.; Bryndin, D.; Bozin, E. S.; Bloch, J.; Proffen, T.; Billinge, S. J., PDFfit2 and PDFgui: computer programs for studying nanostructure in crystals. *J. Phys. Condens. Matter* **2007,** *19*, 335219.
(6） Tucker, M. G.; Keen, D. A.; Dove, M. T.; Goodwin, A. L.; Hui, Q., RMCProfile: reverse Monte Carlo for polycrystalline materials. *J. Phys. Condens. Matter* **2007,** *19*, 335218.
(7） Keen, D. A., A comparison of various commonly used correlation functions for describing total scattering. *J. Appl. Crystallogr.* **2001,** *34*, 172-177.
(8） Hui, Q.; Dove, M. T.; Tucker, M. G.; Redfern, S. A. T.; Keen, D. A., Neutron total scattering and reverse Monte Carlo study of cation ordering in $Ca_xSr_{1-x}TiO_3$. *J. Phys. Condens. Matter* **2007,** *19*, 11.